
Article

Establishment of a Dual-Reporter Minigenome System for Respiratory Syncytial Virus

Li Pan^{1#}, Yunbo Xu^{2,1#}, Yihan Ma¹, Jiaxing Zhang^{3,4,1}, Chao Wu^{1,3*}

1 Institute of Systems and Physical Biology, Shenzhen Bay Laboratory, Shenzhen, China.
2 School of Life Science and Technology, Harbin Institute of Technology, Harbin, China.
3 Shenzhen Medical Academy of Research and Translation (SMART), Shenzhen 518107, China
4 Westlake University, Hangzhou 310030, China
These authors contributed equally
* Correspondence: wuchao@szbl.ac.cn (C.W.)

Abstract

Respiratory syncytial virus (RSV) poses a significant global health challenge, particularly affecting infants, the elderly, and immune compromised individuals. Despite recent progress in the development of vaccines and monoclonal antibodies, effective antiviral therapies remain limited. To advance the discovery of antiviral drugs, we have developed a dual-reporter RSV minigenome system, providing a safe and robust platform for antiviral evaluation. This system incorporates NanoLuc luciferase and superfolder GFP (sfGFP) linked by a self-cleaving P2A peptide, allowing for simultaneous detection of orthogonal signals. Validation with L polymerase inhibitors confirmed the system's reliability for screening small-molecule inhibitors. The linear correlation observed between reporter signals enhances the assay's reliability for antiviral assessment. This dual-reporter minigenome system advances targeted therapeutic strategies against RSV.

Keywords: Respiratory Syncytial Virus, Minigenome, Dual-reporter system, Antiviral drug evaluation, Large polymerase

1. Introduction

Respiratory Syncytial Virus (RSV) poses a significant global health risk, especially to infants, the elderly, and those with weakened immune systems [1]. It is a leading cause of lower respiratory infections in infants, with millions of cases annually, mainly in resource-limited countries [2, 3]. In adults, particularly the elderly, RSV is a major cause of severe respiratory illness [4]. The virus can lead to pneumonia and other serious complications, especially in immunocompromised individuals [5]. There is increasing focus on developing vaccines and antiviral treatments to address RSV's impact across all age groups [6, 7]. Despite extensive research, significant obstacles remain in developing RSV interventions. Vaccine candidates struggle with less than 75% efficacy in elderly trials, limited age-specific use, and incomplete protection against diverse strains [8-10]. Similarly, antiviral development remains restricted, with only three FDA-approved agents—the small-molecule inhibitor ribavirin and the monoclonal antibodies palivizumab and nirsevimab—offering limited effectiveness against evolving variants [11] and the antiviral drug market is projected to reach \$2.5 billion by 2030 [10, 12]. Antiviral drug discovery using wild-type or recombinant viruses is technically complex, time-consuming, and requires strict biosafety measures. Minigenome platforms offer a solution without using infectious viral particles, reducing biosafety risks and speeding up drug discovery [12]. Complementary structure-guided approaches such as fragment-based screening have

also been used to target conserved nucleoprotein domains implicated in viral RNA synthesis, providing starting points for small-molecule development [13].

The minigenome system is a powerful tool in virology, enabling researchers to dissect viral replication and transcription in cellular contexts without viral infection [14, 15]. This system typically employs truncated viral genomic or antigenomic cDNA fragments, in which most viral genes are replaced with reporter genes. This substitution allows recapitulation of viral processes through the expression of readily detectable markers, such as luciferase or fluorescent proteins [14]. Minigenome platform helps evaluate potential viral RNA synthesis inhibitors [16, 17] and identify essential proteins and RNA elements for viral processes like genome encapsulation and transcriptional regulation [15, 18]. The use of minigenome system to study filovirus replication and transcription has also been demonstrated [19-21]. For example, Ebola virus minigenome assays have been applied to functionally map nucleoprotein determinants and to test inhibitory strategies targeting key protein interfaces [22, 23].

RSV gene expression has been examined using several complementary reconstituted systems that differ in how much of the viral life cycle they model. A widely used helper-dependent dicistronic minigenome (e.g., RSV-CAT-LUC) is transfected as *in vitro*-synthesized RNA into RSV-infected cells, where the infection supplies the viral factors needed for transcription/replication, making it particularly useful for testing how different intergenic regions influence sequential transcription [14]. In contrast, infection-free minigenome assays reconstitute RSV polymerase activity by co-expressing the required viral components alongside a reporter minigenome, enabling quantitative analysis of transcription (and, depending on design, genome replication) without the confounding effects of infection [24]. A more reductionist minimal replication system demonstrated that functional expression of N, P, and L from cDNA is sufficient to support replication of RSV genomic RNA analogs, thereby defining the minimal trans-acting requirements for RNA replication [25]. Finally, full reverse genetics platforms (e.g., BAC-stabilized RSV antigenome cDNA combined with recombination-mediated mutagenesis) allow hypotheses from minigenome assays to be validated in the context of infectious recombinant RSV [26].

Building upon these foundations, we engineered a dual-reporter minigenome system capable of simultaneously expressing NLuc luciferase and sfGFP. This design integrates orthogonal detection modalities into a single platform to ensure robust data reliability. While NLuc offers superior sensitivity and dynamic range for high-throughput biochemical quantification, sfGFP provides a critical validation layer through real-time spatial visualization and flow cytometry [27]. Importantly, this dual-readout strategy effectively mitigates false-positive hits common in high-throughput screening—specifically those caused by compounds that directly inhibit luciferase enzymatic activity or stability rather than viral replication—thereby significantly enhancing the fidelity of antiviral drug discovery.

2. Materials and Methods

2.1. Viruses, cells and plasmids

The RSV A2 strain was obtained from the Chinese Academy of Medical Sciences Collection Center for Pathogenic Microorganisms. The BSR-T7/5 and HEp-2 cell lines were maintained in DMEM medium supplemented with 10% fetal bovine serum (FBS) at 37°C in a 5% CO₂ atmosphere. Furthermore, we constructed expression plasmids encoding the N, P, M2-1, and L proteins of the RSV A2 strain, specifically pCAGGS(+)-RSV A2-N, pCAGGS(+)-RSV A2-P, pCAGGS(+)-RSV A2-M2-1, and pCAGGS(+)-RSV A2-L. The primers employed for RT-qPCR were as follows: forward primer

RGGAATGCTTCACACATTAGT and reverse primer CCTCATTCTGACTCTGCC. 94
We created RSV L active site mutant plasmids named L-D811A, L-G1264A, L-R1339A, and 95
L-G1855S based on published papers or articles [29, 30], and confirmed their sequences 96
through sequencing. 97

2.2. Construction of minigenomes 98

The reporter gene is flanked by the RSV gene start (GS) and gene end (GE) sequences, 99
which play a crucial role in regulating expression. To more accurately simulate viral 100
replication, non-coding regions (NC), such as NS1-NC and L-NC, are inserted adjacent to 101
the GS and GE sequences [31]. Furthermore, the minigenome complementary DNA 102
(cDNA) incorporates Leader and Trailer sequences, along with the T7 promoter, T7 103
terminator, and ribozymes (e.g., hammerhead ribozyme [HHRz] and hepatitis delta virus 104
ribozyme [HDVRz]) [32, 33]. The Leader and Trailer sequences are responsible for 105
transcription and replication, while the ribozymes ensure precise terminal sequence for 106
both positive and negative strand minigenomes [34]. Transcription from the T7 promoter 107
is facilitated by T7 RNA polymerase (T7 RNP), which is provided through recombinant 108
viruses, expression plasmids, or genetically engineered cell lines [15]. The T7 terminator 109
ensures precise termination of transcription downstream of the viral genome. In order to 110
replicate the negative-sense RNA genome of RSV, all non-structural elements, including 111
the T7 promoter, terminator, and ribozymes, were strategically engineered in a reverse 112
complementary orientation. We developed three distinct minigenome constructs: (1) a 113
system expressing NLuc, (2) a system expressing sfGFP and (3) a dual-reporter system 114
facilitating co-expression of NLuc and sfGFP fused with a self-cleaving peptide P2A. 115

Design Specifications: 116

(A) Mini-NLuc: 5'-T7 pro→HHRz→Trailer→L GE→NC2→NLuc→NC1→NS1
GS→Leader→HDVRz→T7 ter; 117
(B) Mini-sfGFP: 5'-T7 pro→HHRz→Trailer→L GE→NC2→sfGFP→NC1→NS1
GS→Leader→HDVRz→T7 ter; 118
(C) Mini-NLuc-sfGFP: 5'-T7 pro→HHRz→Trailer→L
GE→NC2→sfGFP→P2A→NLuc→NC1→NS1 GS→Leader→HDVRz→T7 ter. 119

A critical feature of the dual-reporter design is the incorporation of the P2A peptide, 120
which facilitates the coordinated translation of both reporter proteins from a single mRNA 121
transcript via ribosomal skipping. The cDNA sequences were synthesized by General 122
Biology (Anhui) Co., Ltd., and subsequently cloned into the pOK12 vector to construct the 123
pOK12-Mini-NLuc, pOK12-Mini-sfGFP, and pOK12-Mini-NLuc-sfGFP plasmids. The 124
plasmids were sequenced by BGI Biological Engineering (Shenzhen) Co., Ltd. 125

2.3. Transfection system 129

BSR-T7/5 cells were cultured in 12-well plates and transfected with Lipofectamine 130
2000 (Thermo Fisher Scientific, catalog# 11668019) upon reaching 80–90% confluency. The 131
optimized transfection are detailed in Table 1. At 48 hours post-transfection, sfGFP 132
expression levels were quantified via fluorescence microscopy, while NanoLuc luciferase 133
activity was evaluated using the Nano-Glo® Dual-Luciferase® Reporter Assay System 134
(Promega, catalog number N1620), following the manufacturer's protocol. FLuc was 135
introduced as a transfection control [35]. 136

Table1: Minigenome transfection protocol 137

Groups	Shared plasmids	Additional Plasmids
--------	-----------------	---------------------

I	Mini-NLuc-sfGFP (1 µg) +pCAGGS-RSV A2-L (1 µg)	
II	Mini-NLuc-sfGFP (1 µg)	
III	pCAGGS-RSV A2-N (0.5 µg) pCAGGS-RSV A2-P (0.5 µg)	Mini-NLuc (1 µg) +pCAGGS-RSV A2-L (1 µg)
IV	pCAGGS-RSV A2-M2-1 (0.5 µg) pcDNA3.1(+)-FLuc (0.5 µg)	Mini-NLuc (1 µg)
V		Mini-sfGFP (1 µg) +pCAGGS-RSV A2-L (1 µg)
VI		Mini-sfGFP (1 µg)
		140
<i>2.4. Small molecule compounds evaluation</i>		141
Small molecule inhibitors of RSV L polymerase, AVG-233 (CAS no. 2151937-80-1) and RSV L-protein-IN-4 (CAS no. 851657-60-8), both sourced from Topscience Co. Ltd, China, were diluted in DMSO to create stock solutions at various concentrations. Cytotoxic effects of these compounds were assessed on BSR T7/5 and HEp-2 cell lines, and the maximum non-toxic dose was determined. Subsequently, BSR-T7/5 cells were cultured and seeded into a 12-well plate. Once cell confluence reached 80%–90%, transfection was conducted using Lipofectamine 2000 reagent. Six hours post-transfection, medium was replaced with fresh one containing varying concentrations of small molecules. Samples were incubated at 37°C in a 5% CO ₂ atmosphere for 48 hours. Control groups, transfected with minigenome plasmids and treated with DMSO (vehicle control), were assayed for Fluc activity.	142 143 144 145 146 147 148 149 150 151 152	
<i>2.5. Correlation analysis of NLuc and sfGFP reporter signal</i>		153
Inhibitory effects of t AVG-233 and RSV L-protein-IN-4 on expression of sfGFP and NLuc from Mini-NLuc-sfGFP were tested. An inverted fluorescence microscope was used to observe sfGFP expression, and the fluorescence intensity of sfGFP was analyzed using Fiji (Image J) software (https://fiji.sc/). Meanwhile, the luciferase activity of treatment groups was determined. Finally, the measured sfGFP fluorescence intensity data and luciferase activity data were fitted with a linear function.	154 155 156 157 158 159	
<i>2.6. Assessment of small molecule inhibitors on RSV replication</i>		160
HEp-2 cells were cultivated in 12-well plates until t 90% confluence. Viral load was calibrated by performing cell counts across triplicate wells. Cells were subsequently infected with the RSV A2 (MOI 0.1) for 2 hours at 37°C. Following the adsorption phase, unbound virions were eliminated by performing three washes with serum-free DMEM. Treatment groups were then administered a maintenance medium containing 2% FBS with varying concentrations of AVG-233 or RSV L-protein-IN-4, and incubated for 72 hours.	161 162 163 164 165 166 167	
To assess the inhibitory effects of small molecules on RSV A2 replication, immunofluorescence staining was performed. Initially, cells were washed with PBS to remove serum and subsequently fixed with 4% paraformaldehyde (Cat# P0099-500mL, Beyotime) for 30 minutes at room temperature. Following three PBS washes, cells were permeabilized with 0.3% Triton X-100 (Cat# P0096-100mL, Beyotime) for 5 minutes, followed by three additional 5-minute PBS washes. Primary antibody staining was conducted using a 1:500 dilution of mouse anti-RSV N monoclonal antibody (Cat# ab94806, Abcam), with incubation at 4°C for 16 hours. After unbound antibodies were removed through three PBS washes, cells were incubated with a 1:500 dilution of FITC-conjugated goat anti-mouse IgG secondary antibody (Cat# SF131, Solarbio) at room	168 169 170 171 172 173 174 175 176 177	

temperature for 1.5 hours, followed by three final PBS washes. Fluorescent signals were acquired using an inverted fluorescence microscope.

To quantitatively evaluate the impact of small molecules on the replication of the RSV A2 genome, viral genomic RNA was extracted from both the cellular and supernatant fractions of RSV A2-infected cultures treated with varying concentrations of AVG-233 and RSV L-protein-IN-4. This extraction was conducted using a commercial viral DNA/RNA extraction kit (Cat#AG21021, Agbio) following manufacturer's guidelines. Subsequently, reverse transcription-quantitative PCR (RT-qPCR) was performed using RSV P gene-specific primers in conjunction with the One Step RT-qPCR Mix (Cat#Q221-01, Vazyme). Absolute quantification of viral RNA copies was accomplished through use of a pOK12-RSV P plasmid standard curve, facilitating a precise assessment of the inhibition effects mediated by the compounds.

2.7. Statistical analysis

Data analysis was performed using GraphPad Prism 9.0 software. Statistical comparisons were made using Student's two-tailed t-test and two-way ANOVA, with significance set at a p-value < 0.05.

2.8 Schematics

All schematics were created using BioRender software (<https://biorender.com>).

3. Results

3.1. Construction and working principles of the dual-reporter minigenome system

The RSV minigenome system was developed by substituting the viral coding sequences in the genomic cDNA with reporter genes, such as luciferase or fluorescent proteins. This modification was performed while maintaining essential cis-acting elements, specifically the Leader and Trailer sequences, which are crucial for the regulation of transcription and replication.

To develop a multiplexed readout platform, we engineered an advanced dual-reporter minigenome by linking sfGFP and NLuc using a self-cleaving P2A peptide. This configuration facilitates the coordinated expression of both reporters from a single mRNA transcript under a single promoter. The ribosome-skipping activity of the P2A peptide ensures near-complete cleavage of the translated polyprotein, resulting in stoichiometric production of distinct sfGFP and NLuc proteins. The sfGFP reporter was chosen for its remarkable photostability, rapid folding kinetics, and resistance to environmental stressors—characteristics essential for sensitive real-time monitoring in complex biological environments. Concurrently, NLuc luciferase offers superior analytical performance due to its compact size (19.1 kDa), high luminescent output (over 100-fold brighter than firefly luciferase), and rapid signal kinetics, facilitating high-temporal-resolution quantification of viral replication dynamics.

The minigenome functions through a specific mechanism: BSR-T7/5 cells, which stably express T7 RNA polymerase, were co-transfected with an engineered minigenome cDNA and helper plasmids encoding the RSV nucleoprotein (N), phosphoprotein (P), large polymerase (L), and transcription elongation factor (M2-1). Post-transfection, the T7-generated minigenome RNA is encapsidated by N to form a functional ribonucleoprotein template. This RNP is subsequently recognized by the polymerase complex (L and P), aided by M2-1, to initiate transcription of mRNA. This mRNA encodes NLuc and sfGFP, linked by a P2A self-cleaving peptide. During translation, ribosomes synthesize a single NLuc-P2A-sfGFP polyprotein, which undergoes autocatalytic cleavage at the P2A site with approximately 98% efficiency, resulting in the production of discrete, functionally active NLuc and sfGFP proteins. Concurrently with transcription, the polymerase complex facilitates replication by synthesizing antigenomic RNA from the minigenome template, followed by the production of genomic RNA from the antigenomes, thus establishing a self-amplifying replication cycle (Figure 1).

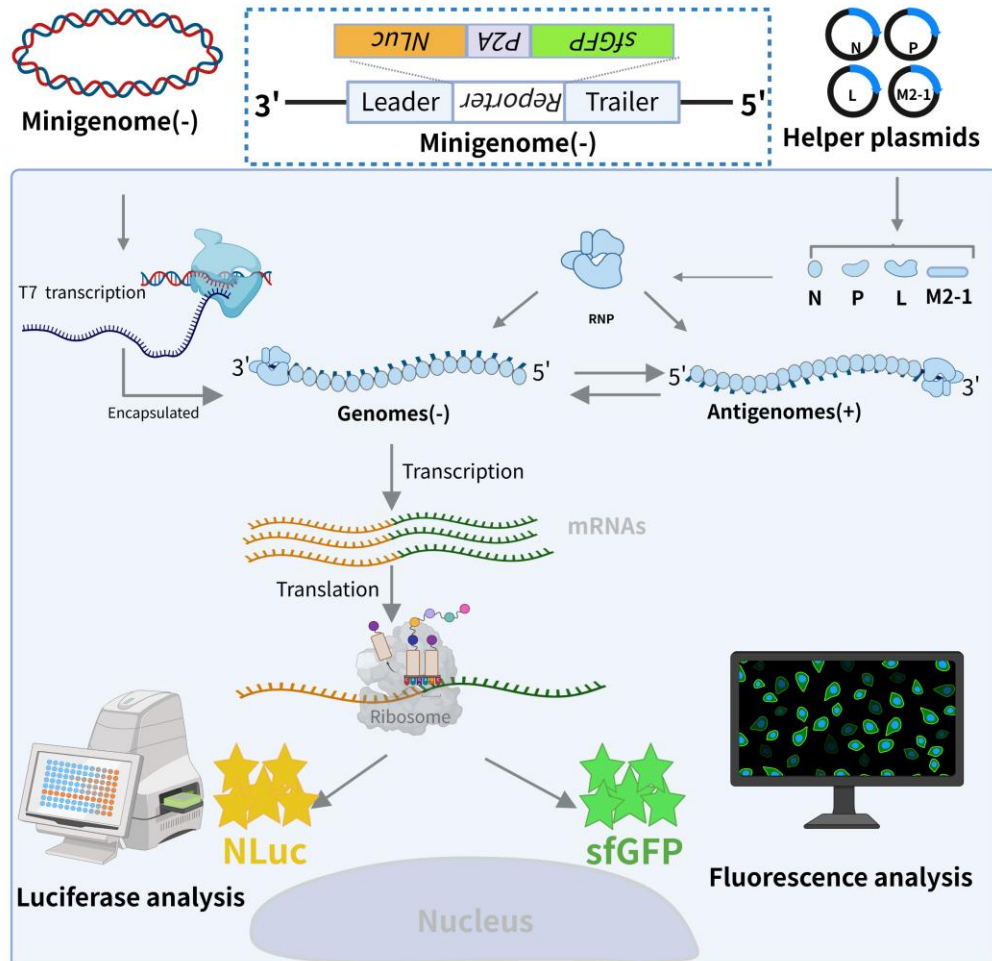


Figure 1. Schematic diagram of the RSV minigenome. The RSV minigenome has been designed as a synthetic analog of the native negative-sense RNA genome, preserving three essential regulatory elements: the Leader sequence, which initiates transcription; the Trailer sequence, which facilitates genome replication; and a dual-reporter cassette. This cassette incorporates sfGFP and NLuc, separated by P2A peptide, thus allowing for equimolar co-expression from a single transcriptional unit.

3.2. The Mini-NLuc and Mini-sfGFP systems exhibit reporter activity

Initially, two minigenome constructs, designated as Mini-NLuc and Mini-sfGFP, were developed in accordance with the experimental design. The Mini-NLuc system incorporates NLuc as its reporter gene, whereas the Mini-sfGFP system utilizes sfGFP as the reporter gene (Figure 2A). To evaluate their functionality, either Mini-sfGFP or Mini-NLuc was co-transfected into BSR-T7/5 cells along with four plasmids encoding the essential auxiliary proteins of the RNP complex: RSV N, P, L, and M2-1 proteins. These proteins are crucial for the transcription and replication of the minigenome. After 48 hours, sfGFP fluorescence was detected via fluorescence microscopy, and luciferase activity was quantified. The results demonstrated robust green fluorescence in cells transfected with Mini-sfGFP (Figure 2B) and significant luciferase activity in cells transfected with Mini-NLuc (Figure 2C), thereby confirming efficient reporter gene expression facilitated by the helper protein complex. Control experiments underscored the critical role of the RSV L protein, as its absence resulted in neither sfGFP fluorescence nor luciferase activity.

Subsequently, the engineered L mutants were assessed utilizing mini-NLuc and mini-sfGFP assays (Figure 2D). Our findings indicate that, in comparison to the wild-type L, the sfGFP fluorescent foci associated with the L active site mutants exhibited a

significant reduction (Figure 2E and F), while NLuc activity was also markedly diminished (Figure 2G). 253
254

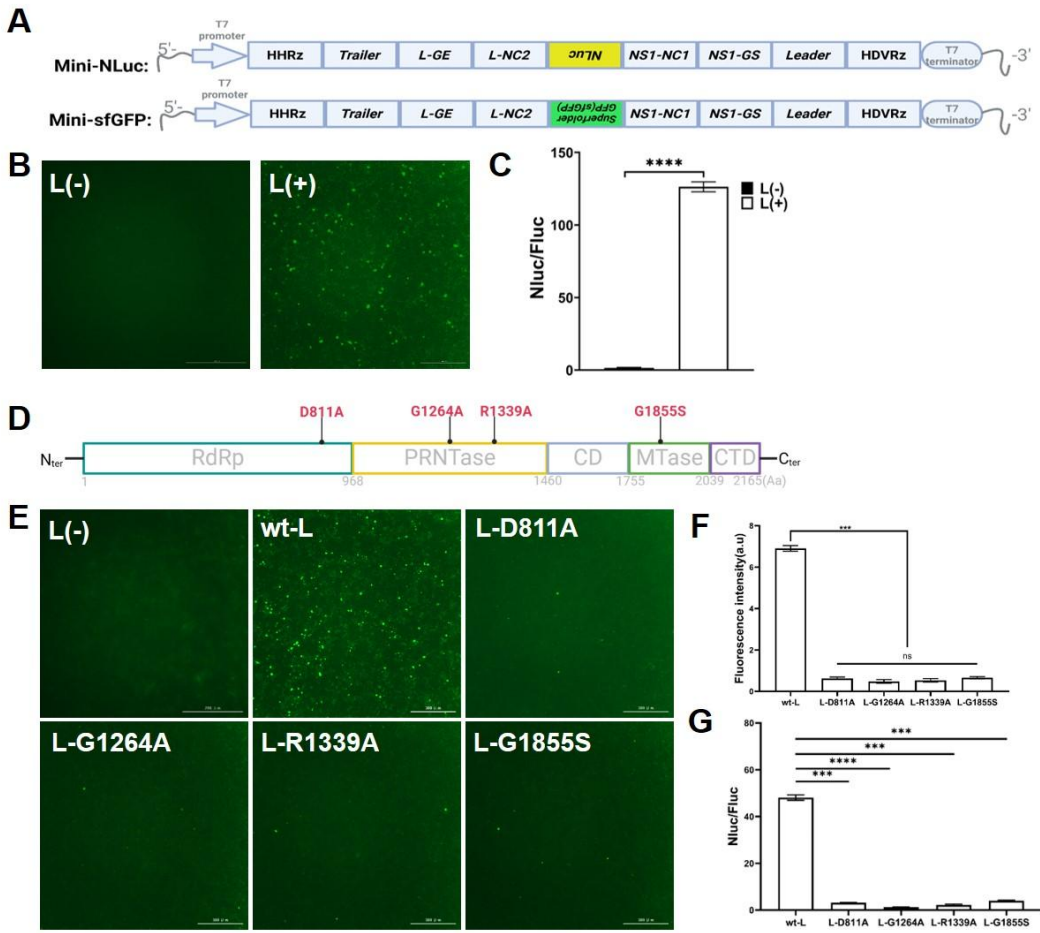


Figure 2. Construction and characterization of the single-reporter gene minigenome. We engineered minigenomes incorporating either NLuc or sfGFP reporter genes to evaluate their functionality through fluorescence and luciferase assays. (A) The Mini-NLuc and Mini-sfGFP vectors are structurally identical except for the reporter gene, with Mini-NLuc comprising the T7 promoter, HHRz, RSV trailer, L gene termination sequence, non-coding regions, NLuc sequence, RSV leader, HDVRz, and T7 terminator. Italicized sequences indicate reverse sequences. (B) Co-transfection of Mini - sfGFP with helper plasmids into BSR T7/5 cells results in green fluorescence, which is absent without the L protein. Scale bar = 300 μ m. (C) Co-transfection of Mini-NLuc with helper plasmids into BSR T7/5 cells induces NLuc activity, which is not observed without the L protein. (D) Diagram of L mutants; (E and F) Analysis of fluorescent foci and fluorescence intensity of L active site mutants using mini-sfGFP. (G) NLuc activity evaluation of L active site mutants via mini-NLuc analysis (** p \leq 0.01; *** p $<$ 0.001). Data are presented as mean \pm SD of three independent experiments, each performed in triplicate. 255
256
257
258
259
260
261
262
263
264
265
266
267
268

3.3. Mini-NLuc-sfGFP co-expresses sfGFP and NLuc

We engineered the dual-reporter minigenome, Mini-NLuc-sfGFP, which integrates benefits of Mini-NLuc and Mini-sfGFP. This construct facilitates the concurrent expression of sfGFP and NLuc through a P2A peptide linker (Figure 3A). For functional evaluation, Mini-NLuc-sfGFP was co-transfected with plasmids encoding the RSV N, P, L, and M2-1 proteins into BSR-T7/5 cells. At 48 hours post-transfection, both sfGFP fluorescence and NLuc activity were assessed. The results indicated that sfGFP expression in Mini-NLuc-sfGFP-transfected cells was comparable to that in Mini-sfGFP-transfected cells (Figures 3B, 3C), and NLuc activity was analogous to that observed in Mini-NLuc-transfected cells (Figure 3D). These findings confirm that Mini-NLuc-sfGFP successfully

integrates the functionalities of both single-reporter systems, facilitating efficient co-expression of sfGFP and NLuc without compromising the performance of either reporter.

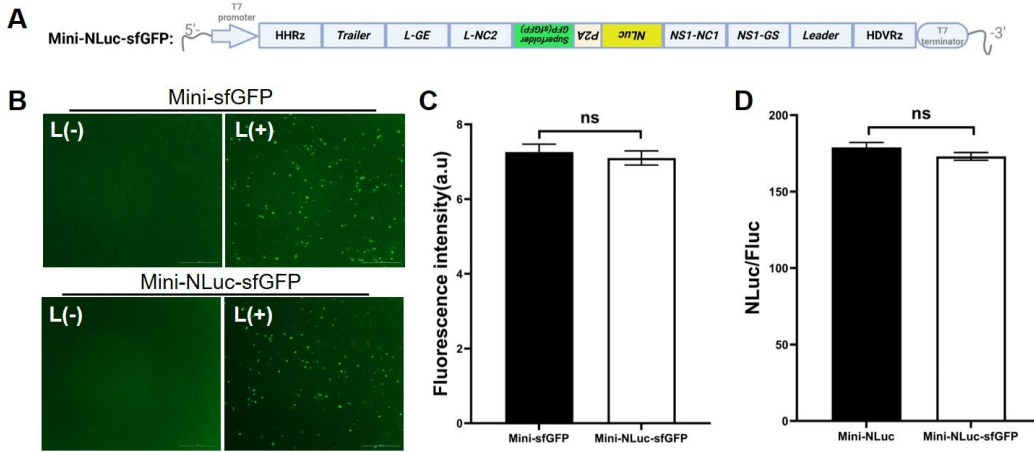


Figure 3. Construction and characterization of Mini-NLuc-sfGFP. (A) Mini-NLuc-sfGFP's structure includes the T7 promoter, HHRz sequence, trailer, L gene end signal and untranslated regions, NLuc sequence, NS1 gene untranslated and gen start signal, leader region, HDVRz sequence, and T7 terminator. Italicized sequences indicate reverse sequences. (B) Co-transfection with helper plasmids in BSR-T7/5 cells produced green fluorescent spots, absent without L (scale bar: 300 μ m). (C) sfGFP fluorescence in Mini-NLuc-sfGFP-transfected cells match that of Mini-sfGFP-transfected cells. (D) Luciferase activity was present in cells co-transfected with Mini-NLuc-sfGFP and helper plasmids, but absent without the L protein. Data are presented as mean \pm SD of three independent experiments, each performed in triplicate.

3.4. Mini-NLuc-sfGFP is an efficient tool for evaluating antiviral small molecules

The Mini-NLuc-sfGFP system was employed to evaluate small molecules for antiviral activity against RSV, with AVG-233 and RSV L protein-IN-4 selected as test compounds (Figures 4A). Initially, BSR-T7/5 cells were co-transfected with plasmids encoding the RSV proteins N, P, L, and M2-1. Subsequently, AVG-233 and RSV L protein-IN-4 were added individually, and after a 48-hour incubation period, their capacity to inhibit minigenome expression was assessed by monitoring sfGFP fluorescence intensity and measuring NLuc activity. The results indicated that both compounds significantly reduced NLuc activity in a dose-dependent manner (Figures 4B and 4C), underscoring the practical utility of this system for preliminary antiviral evaluation. Based on these findings, subsequent experiments will employ lower concentrations of the compounds to further explore their inhibitory effects on reporter gene signals.

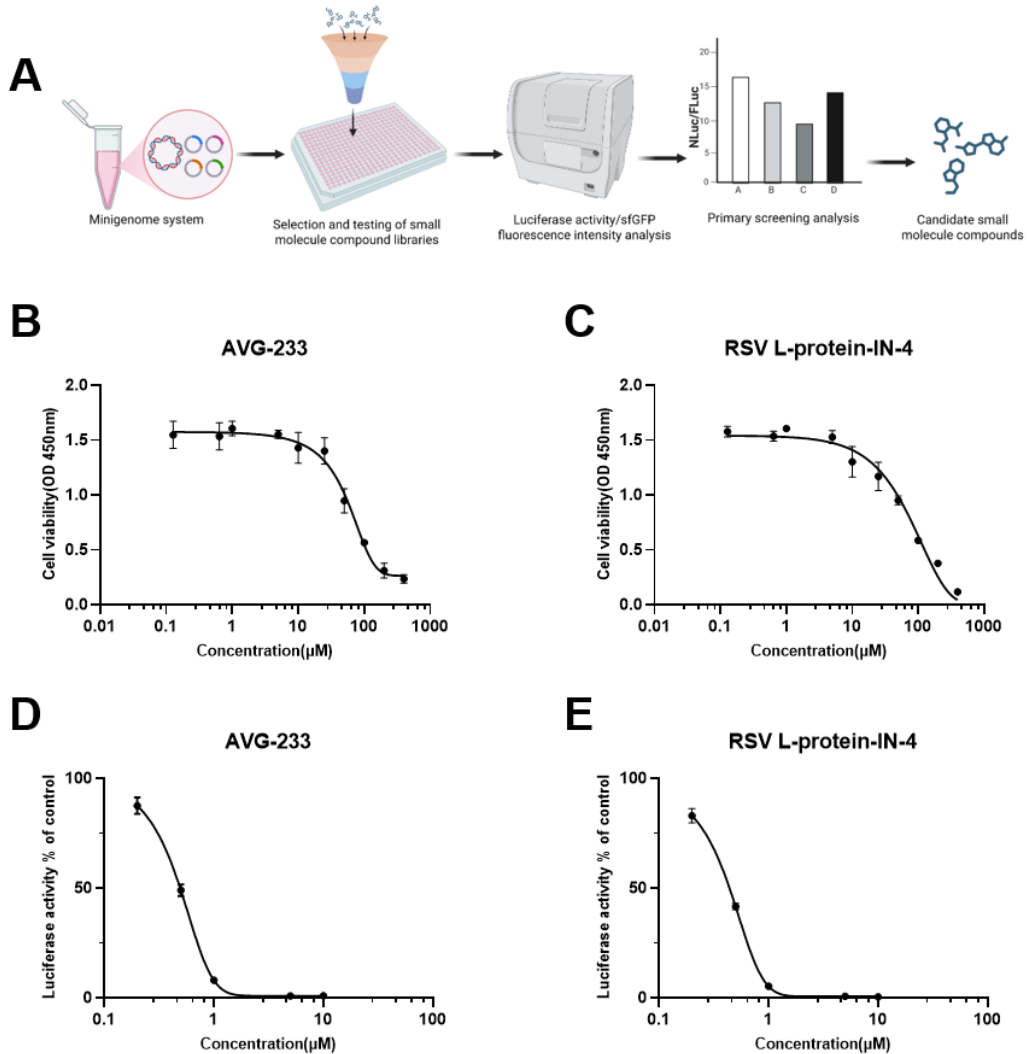


Figure 4. Mini-NLuc-sfGFP for small molecule evaluation. (A) The experimental protocol involved transfected the Mini-NLuc-sfGFP minigenome into BSR-T7/5 cells, followed by treatment with a range of small molecules. The inhibitory effects were initially assessed by quantifying fluorescence intensity or NLuc activity, leading to the selection of promising candidates for further investigation. (B) AVG-233 reduced BSR-T7/5 cell viability in a concentration-dependent manner (OD₄₅₀). (C) Similarly, RSV L-protein-IN-4 reduced BSR-T7/5 cell viability in a concentration-dependent manner (OD₄₅₀). (D) AVG-233 demonstrated a dose-dependent inhibition of Mini-NLuc-sfGFP reporter gene expression, as indicated by luciferase activity. (E) Similarly, RSV L-protein-IN-4 exhibited dose-dependent inhibition of Mini-NLuc-sfGFP reporter gene expression, also measured by luciferase activity. Data are presented as mean \pm SD of three independent experiments, each performed in triplicate.

3.5. Mini-NLuc-sfGFP shows a linear correlation between NLuc and sfGFP signals

We assessed the linear relationship between sfGFP fluorescence and NLuc activity in the Mini-NLuc-sfGFP system by examining the effects of two RSV L protein inhibitors, AVG-233 and RSV L-protein-IN-4. Both inhibitors were tested across a range of concentrations, with measurements taken for sfGFP fluorescence and NLuc activity. The results indicated that AVG-233 induced dose-dependent reductions in both sfGFP fluorescence (Figure 5A and B) and NLuc activity (Figure 5C), demonstrating a strong linear correlation ($R^2 = 0.977$, Figure 5D). Similarly, RSV L-protein-IN-4 led to dose-dependent decreases in sfGFP fluorescence (Figure 6A and B) and NLuc activity (Figure 6C), also exhibiting a strong linear correlation ($R^2 = 0.974$, Figure 6D). In conclusion, the Mini-NLuc-sfGFP system effectively produces concurrent sfGFP and NLuc signals with a

303
304
305
306
307
308
309
310
311
312
313
314
315
316
317
318
319
320
321
322
323
324
325

robust linear relationship, underscoring its reliability for screening antiviral compounds against RSV and supporting future drug development endeavors.

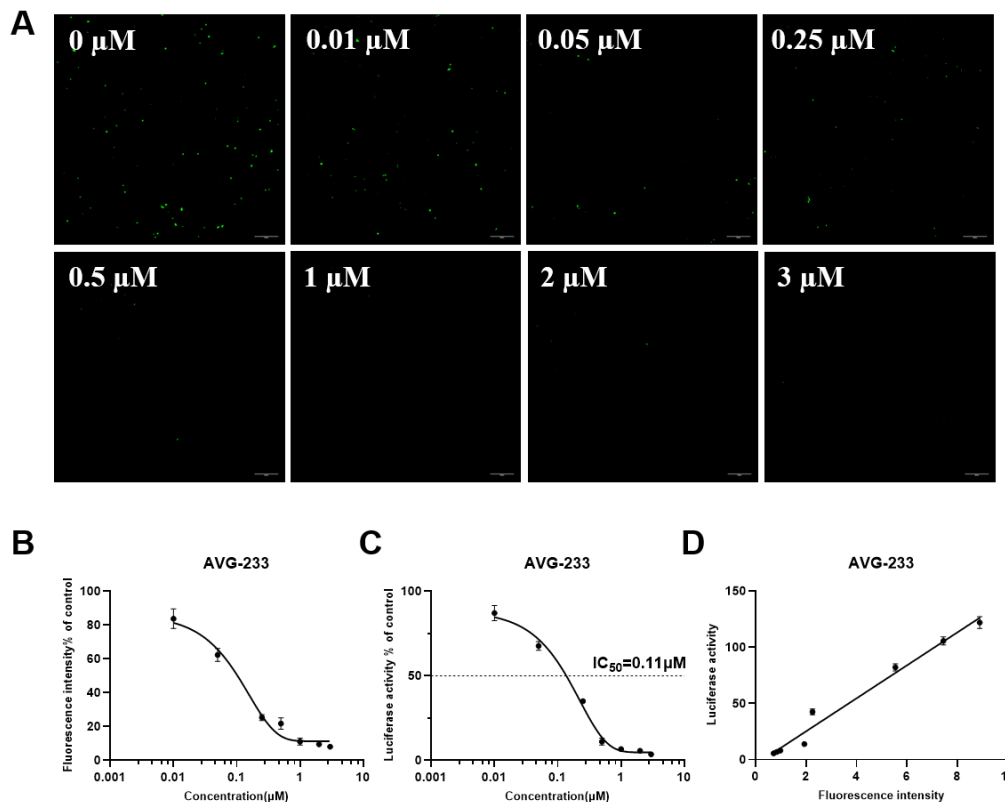


Figure 5. Analysis of the linear relationship between sfGFP and NLuc in Mini-NLuc-sfGFP for evaluating AVG-233. (A) Effect of AVG-233 on sfGFP fluorescence at 0, 0.01, 0.05, 0.25, 0.5, 1, 2, and 3 μM . (B and C) AVG-233 demonstrated a dose-dependent inhibition of Mini-NLuc-sfGFP reporter gene expression, as indicated by fluorescence intensity and luciferase activity. (D) Linear regression showed a significant correlation between sfGFP and NLuc. Scale bar: 400 μm . Data are presented as mean \pm SD of three independent experiments, each performed in triplicate.

326
327

328
329
330
331
332
333
334

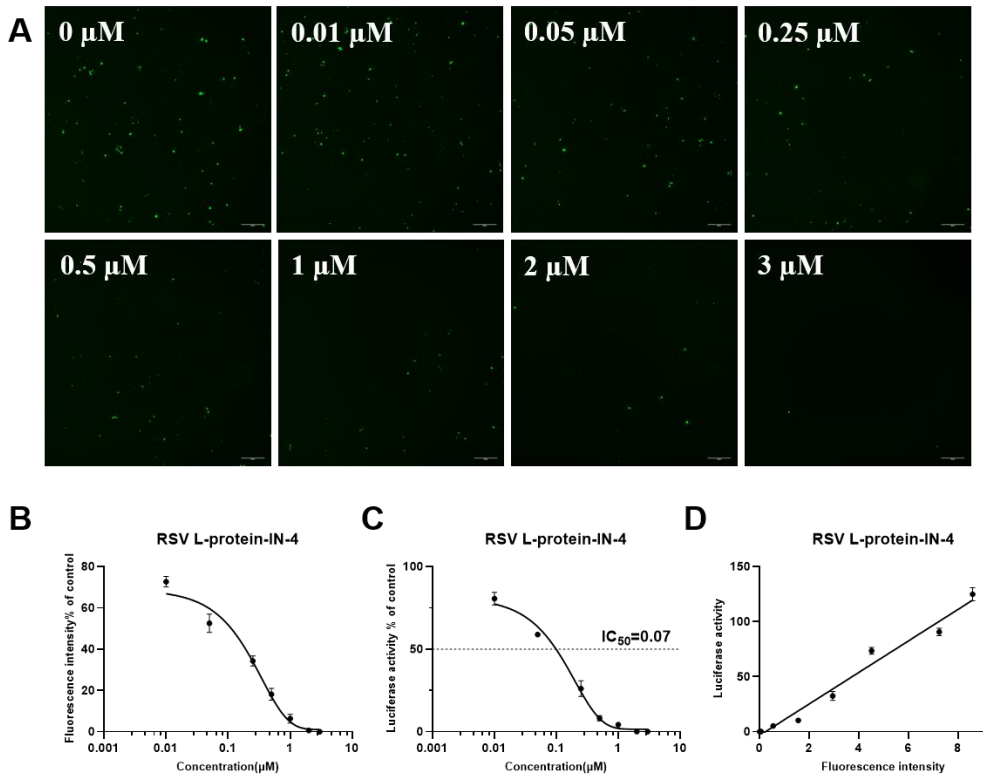


Figure 6. Analysis of the linear relationship between sfGFP and NLuc in Mini-NLuc-sfGFP for evaluating RSV L-protein-IN-4. (A) Effect of RSV L-protein-IN-4 on sfGFP fluorescence at 0, 0.01, 0.05, 0.25, 0.5, 1, 2, and 3 μM. (B and C) RSV L-protein-IN-4 demonstrated a dose-dependent inhibition of Mini-NLuc-sfGFP reporter gene expression, as indicated by fluorescence intensity and luciferase activity. (D) Linear regression showed a significant correlation between sfGFP and NLuc. Scale bar: 400 μm. Data are presented as mean ± SD of three independent experiments, each performed in triplicate.

3.6. Mini-NLuc-sfGFP strongly correlates with viral inhibition in small molecule evaluations

To validate the Mini-NLuc-sfGFP system for assessing small-molecule inhibitors of RSV replication, we evaluated two compounds—AVG-233 and RSV L-protein-IN-4—both known to target the RSV L protein. Their inhibitory effects across concentrations were analyzed using indirect immunofluorescence assays (IFA) and reverse transcription quantitative PCR (RT-qPCR).

Results showed that increasing concentrations of AVG-233 (Figure 7A) and RSV L-protein-IN-4 (Figure 7C) reduced viral infection foci. RT-qPCR further confirmed dose-dependent suppression of wild-type RSV A2 genome replication: AVG-233 reduced viral genome copies from 0 to 3 μM (Figure 7C), whereas RSV L-protein-IN-4 inhibited replication within its safe concentration range (Figure 7D).

The integration of IFA and RT-qPCR facilitated a thorough examination of the antiviral efficacy and dose-dependency of the compounds, thereby affirming a robust correlation between the Mini-NLuc-sfGFP system and live virus.

335
336
337
338
339
340
341
342
343
344
345
346
347
348
349
350
351
352
353
354
355
356

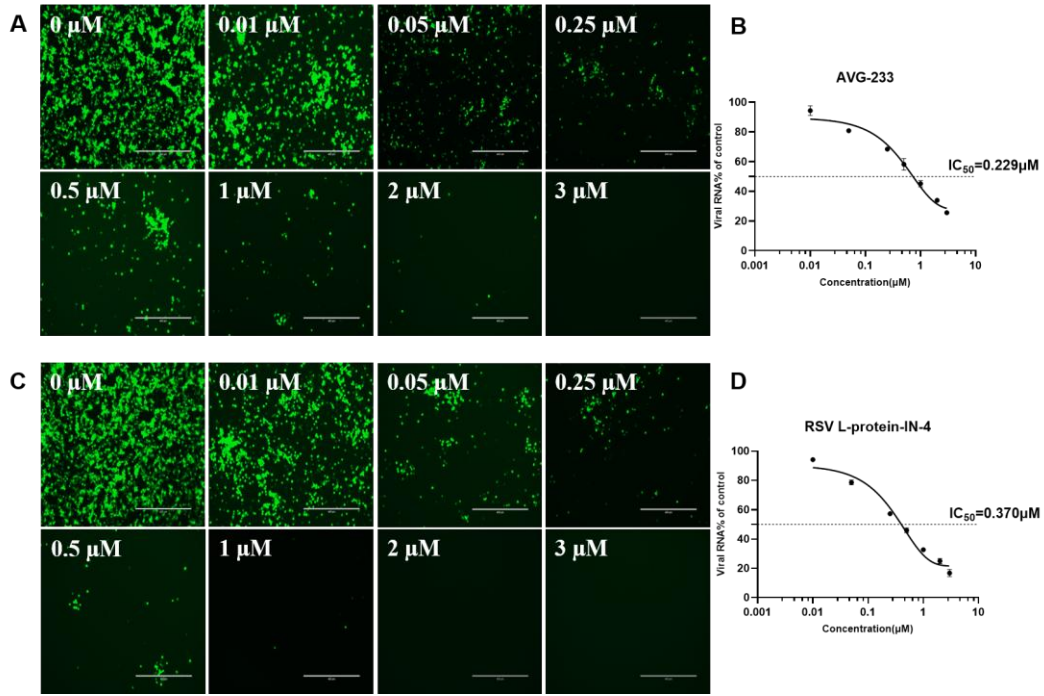


Figure 7. Validation of small-molecule inhibitory effects assessed by Mini-NLuc-sfGFP and confirmed in RSV A2. RSV A2 infection was conducted at a multiplicity of infection (MOI) of 0.1, utilizing a primary antibody of mouse anti-RSV F and a secondary antibody of goat anti-mouse FITC conjugate (A) Immunofluorescence imaging showed that AVG-233 inhibited viral infection at 0, 0.01, 0.05, 0.25, 0.5, 1, 2, and 3 μM. (B) Viral genome copy numbers via RT-qPCR at equivalent concentrations. (C) Immunofluorescence imaging showed that RSV L-protein-IN-4 inhibited viral infection at 0, 0.01, 0.05, 0.25, 0.5, 1, 2, and 3 μM. (D) Viral genome copy numbers via RT-qPCR at equivalent concentrations. Scale bar: 400 μm. Data are presented as mean ± SD of three independent experiments, each performed in triplicate.

4. Discussion

RSV affects people of all ages, with children, the elderly, and those with weakened immune systems being most at risk [36]. Although there are no global antiviral treatments for RSV, the FDA approved two vaccines in 2023 [37]. However, the FDA and CDC have warned that these vaccines might increase the risk of Guillain-Barré syndrome in older adults [38, 39]. RSV small molecule inhibitors show promise as targeted therapies for high-risk groups, such as newborns, the elderly, and those with weakened immune systems, including cancer patients and organ transplant recipients [40, 41]. After the zero-COVID policy was optimized in late 2022, RSV cases surged in Northern China, with the winter 2023 peak reaching a nine-year high [42]. This underscores the ongoing challenges in managing RSV and the urgent need for effective treatments.

Traditional RSV minigenome systems rely on BSR T7/5 cells or recombinant vaccinia viruses to provide T7 RNA polymerase. However, vaccinia-based methods can be unstable and introduce interfering viral components. In contrast, the Mini-NLuc-sfGFP system works efficiently in BSR T7/5 cells, which already express T7 RNA polymerase [43]. This system, which integrates fluorescence and luciferase reporters, facilitates both qualitative and quantitative evaluation of small molecules, thereby supporting drug screening and efficacy assessment. Notably, related filovirus minigenome reporter assays have been implemented in a 96-well, internally normalized dual-luciferase format, illustrating feasibility for scalable reporter-based testing [28]. Beyond its application in drug discovery, the dual-reporter minigenome serves as a crucial tool for investigating viral protein functions and replication, thereby advancing our comprehension of RSV biology and aiding in the development of antiviral strategies [44]. Additionally, it forecasts the success of recombinant virus rescue, thereby enhancing experimental

outcomes and timelines [26]. As demonstrated in Figure 2, L mutants led to a marked decrease in reporter signals. The application of this minigenome system permits an initial evaluation of the impact of key RSV gene mutations on protein function. This methodology not only conserves time by obviating the need for recombinant virus construction but also contributes to the targeted development of inhibitors. The system's strong compatibility and linearity of reporter signals improve accuracy and reliability. A P2A sequence between sfGFP and NLuc genes enables efficient co-expression from one mRNA, enhancing system efficiency. We chose sfGFP and NLuc for their brightness, rapid folding, stability, low background fluorescence, and quick response, making them ideal for early signal detection and sensitive experiments. This dual-reporter system provides reliable results even under challenging conditions such as temperature or pH fluctuations and toxin exposure, ensuring consistent reporter gene expression [45, 46].

RSV depends on its polymerase complex (N, P, L, and M2-1 proteins) for genome replication [47]. The multifunctional L polymerase is crucial for transcribing viral mRNA and synthesizing complementary RNA, making it a key target for RSV antiviral development [48-50]. Our study used the RSV minigenome system to evaluate two small molecules, AVG-233 and RSV L-protein-IN-4, targeting the L polymerase. AVG-233 non-competitively inhibits RNA synthesis post-initiation, while RSV L-protein-IN-4 blocks mRNA capping, inhibiting mRNA synthesis and viral replication [51, 52]. Both compounds dose-dependently reduced sfGFP and NLuc reporter signals, confirmed in wild-type RSV A2 virus assays, demonstrating the Mini-NLuc-sfGFP system's effectiveness in evaluating RSV-targeting small molecules.

The Mini-NLuc-sfGFP system is used not only to discovery drugs targeting the L polymerase but also to investigate RSV's replication and transcription mechanisms. This includes studying the Leader and Trailer regions' roles in genome replication and the effects of viral proteins like N, P, L, and M2-1 on replication compartment formation. Increased N protein levels boost viral RNA replication, while M2-1 does not affect RNA replication or mRNA to antigenome synthesis ratios[53]. Additionally, research on related viruses, such as Ebola, has utilized minigenomes to characterize RNA editing mechanisms and identify essential cis-acting sequences near the editing site [54]. Another study highlighted that specific basic residues, particularly in the first basic patch, are vital for viral RNA synthesis and replication complex formation, influencing VP35-nucleoprotein interactions [55].These findings indicate that our mini-NLuc-sfGFP system can enhance understanding of RSV replication and transcription mechanisms.

The Mini-NLuc-sfGFP system offers significant benefits but also has limitations and areas for improvement. It's optimized for a stable T7 polymerase-expressing cell line, removing the need for external polymerase delivery, but this limits its use to certain cell types, excluding those relevant to RSV, like human airway epithelial cultures. Future improvements will require alternative polymerase delivery methods. The system's main advantage over single-reporter systems is its built-in internal validation: sfGFP provides quick, spatial, and qualitative feedback on transfection efficiency and minigenome activity, aiding in visual assessment and troubleshooting, while NLuc delivers sensitive, quantitative data ideal for dose-response assays and high-throughput screening.

For most applications, it is advisable to routinely measure both reporters: (1) In the context of drug screening and small-molecule evaluation, NLuc should serve as the primary quantitative readout due to its superior sensitivity, extensive dynamic range, and minimal background interference. The sfGFP signal plays a critical role in quality control, ensuring that any observed reduction in luminescence is attributable to authentic antiviral activity rather than compound cytotoxicity or inadequate transfection, both of which could also lead to diminished GFP fluorescence. We recommend employing sfGFP for rapid primary screening, such as high-throughput visual inspections to eliminate inactive compounds, thereby reducing the number of samples necessitating NLuc quantification. Subsequently, NLuc should be utilized to generate precise IC₅₀ data for identified hit compounds. For long-term assays exceeding 48 hours, it is advisable to prioritize NLuc, as sfGFP may be susceptible to photobleaching or accumulation in lysosomes, which could result in signal saturation. (2) In investigations of viral replication and transcription

mechanisms, the use of sfGFP proves to be invaluable for monitoring the temporal and spatial dynamics of minigenome activity in live cells, while NLuc offers precise kinetic data derived from the same sample lysates. A divergence in the signals from these two reporters should not be interpreted as indicative of system failure; rather, it presents an opportunity for more in-depth analysis. A notable reduction in the NLuc signal, accompanied by a stable sfGFP fluorescence, may imply a specific inhibition of translation or a potential issue with the luciferase assay itself, such as reagent instability. Conversely, a simultaneous loss of both signals strongly suggests a defect in upstream processes, such as RNA synthesis or overall minigenome integrity. Consequently, the dual-reporter system not only enhances the reliability of the data but also provides a more comprehensive toolkit for diagnosing the mechanisms of action of antiviral compounds or the functional consequences of mutations in viral proteins.

Considering these factors, the Mini-NLuc-sfGFP system offers a robust platform for RSV research, supporting both antiviral discovery and fundamental virology. By expanding existing RSV minigenome tools with dual, complementary readouts, it enables efficient evaluation of antiviral candidates and functional analysis of key viral genes.

Author Contributions: Conceptualization, L.P., Y. X and C.W.; methodology, L.P., Y.X., Y.M., J. Z. and C. W.; writing—original draft preparation, L.P., Y.X., J. Z., and C. W.; writing—review and editing, L. P., Y.X., J. Z., and C.W.; funding acquisition, C.W. All authors have read and agreed to the published version of the manuscript.

Author Contributions: Conceptualization, L.P., Y. X and C.W.; methodology, L.P., Y.X., Y.M., J. Z. and C. W.; writing—original draft preparation, L.P., Y.X., J. Z., and C. W.; writing—review and editing, L. P., Y.X., J. Z., and C.W.; funding acquisition, C.W. All authors have read and agreed to the published version of the manuscript.

Funding: We are grateful for the financial support of this work from the following: GuangDong Basic and Applied Basic Research Foundation (2023A1515110369 to C.W.), Guangdong Pearl River Funding (2023QN10Y129 to C. W.), and Shenzhen Bay Laboratory Startup Fund (SZBL21240121 to C.W.).

Informed Consent Statement: Not applicable.

Acknowledgments: We extend our sincere gratitude to the Chinese Academy of Medical Sciences Collection Center for Pathogenic Microorganisms for their generous provision of the RSV A2 strain. Additionally, we are grateful to Dr. Yang Liu and Min Zheng for their contribution of experimental materials and invaluable suggestions. We acknowledge the Shenzhen Medical Academy for providing BSL-2 laboratory support. Finally, we thank Dr. Yang Liu and Daisy W. Leung who critically reviewed the manuscript.

Conflicts of Interest: The authors declare no conflicts of interest.

References

1. Nam, H. H.; Ison, M. G., Respiratory syncytial virus infection in adults. *Bmj* **2019**, 366, l5021.
2. Ruckwardt, T. J.; Morabito, K. M.; Graham, B. S., Immunological Lessons from Respiratory Syncytial Virus Vaccine Development. *Immunity* **2019**, 51, (3), 429–442.
3. Langedijk, A. C.; Bont, L. J., Respiratory syncytial virus infection and novel interventions. *Nat Rev Microbiol* **2023**, 21, (11), 734–749.
4. Wilson, E.; Goswami, J.; Baqui, A. H.; Doreski, P. A.; Perez-Marc, G.; Zaman, K.; Monroy, J.; Duncan, C. J. A.; Ujiie, M.; Rämet, M.; Pérez-Breva, L.; Falsey, A. R.; Walsh, E. E.; Dhar, R.; Wilson, L.; Du, J.; Ghaswalla, P.; Kapoor, A.; Lan, L.; Mehta, S.; Mithani, R.; Panozzo, C. A.; Simorellis, A. K.; Kuter, B. J.; Schödel, F.; Huang, W.; Reuter, C.; Slobod, K.; Stoszek, S. K.; Shaw, C. A.; Miller, J. M.; Das, R.; Chen, G. L., Efficacy and Safety of an mRNA-Based RSV PreF Vaccine in Older Adults. *N Engl J Med* **2023**, 389, (24), 2233–2244.

5. Zar, H. J.; Cacho, F.; Kootbodien, T.; Mejias, A.; Ortiz, J. R.; Stein, R. T.; Hartert, T. V., Early-life respiratory syncytial virus 494
disease and long-term respiratory health. *Lancet Respir Med* **2024**, *12*, (10), 810–821. 495

6. Wildenbeest, J. G.; Lowe, D. M.; Standing, J. F.; Butler, C. C., Respiratory syncytial virus infections in adults: a narrative 496
review. *Lancet Respir Med* **2024**, *12*, (10), 822–836. 497

7. Zhao, S.; Shang, Y.; Yin, Y.; Zou, Y.; Xu, Y.; Zhong, L.; Zhang, H.; Zhang, H.; Zhao, D.; Shen, T.; Huang, D.; Chen, Q.; Yang, 498
Q.; Yang, Y.; Dong, X.; Li, L.; Chen, Z.; Liu, E.; Deng, L.; Jiang, W.; Cheng, H.; Nong, G.; Wang, X.; Chen, Y.; Ding, R.; Zhou, 499
W.; Zheng, Y.; Shen, Z.; Lu, X.; Hao, C.; Zhu, X.; Jia, T.; Wu, Y.; Zou, G.; Rito, K.; Wu, J. Z.; Liu, H.; Ni, X., Ziresovir in 500
Hospitalized Infants with Respiratory Syncytial Virus Infection. *N Engl J Med* **2024**, *391*, (12), 1096–1107. 501

8. Rasmussen, S. A.; Jamieson, D. J., Maternal RSV Vaccine - Weighing Benefits and Risks. *N Engl J Med* **2024**, *390*, (11), 1050– 502
1051. 503

9. Dieussaert, I.; Hyung Kim, J.; Luik, S.; Seidl, C.; Pu, W.; Stegmann, J. U.; Swamy, G. K.; Webster, P.; Dormitzer, P. R., RSV 504
Prefusion F Protein-Based Maternal Vaccine - Preterm Birth and Other Outcomes. *N Engl J Med* **2024**, *390*, (11), 1009–1021. 505

10. Averin, A.; Sato, R.; Begier, E.; Gessner, B. D.; Snow, V.; Cane, A.; Quinn, E.; Atwood, M.; Kijauskaite, G.; Weycker, D., 506
Annual public health and economic burden of medically attended respiratory syncytial virus illnesses among US adults. 507
Vaccine **2024**, *42*, (26), 126323. 508

11. Venkatesan, P., Nirsevimab: a promising therapy for RSV. *Lancet Microbe* **2022**, *3*, (5), e335. 509

12. Hutton, D. W.; Prosser, L. A.; Rose, A. M.; Mercon, K.; Ortega-Sanchez, I. R.; Leidner, A. J.; Havers, F. P.; Prill, M. M.; 510
Whitaker, M.; Roper, L. E.; Pike, J.; Britton, A.; Melgar, M., Cost-effectiveness of vaccinating adults aged 60 years and older 511
against respiratory syncytial virus. *Vaccine* **2024**, *42*, (24), 126294. 512

13. Aceti, D. J.; Ahmed, H.; Westler, W. M.; Wu, C.; Dashti, H.; Tonelli, M.; Eghbalnia, H.; Amarasinghe, G. K.; Markley, J. L., 513
Fragment screening targeting Ebola virus nucleoprotein C-terminal domain identifies lead candidates. *Antiviral Research* 514
2020, *180*, 104822. 515

14. Kuo, L.; Farnes, R.; Collins, P. L., The structurally diverse intergenic regions of respiratory syncytial virus do not modulate 516
sequential transcription by a dicistronic minigenome. *J Virol* **1996**, *70*, (9), 6143–50. 517

15. Radecke, F.; Spielhofer, P.; Schneider, H.; Kaelin, K.; Huber, M.; Dötsch, C.; Christiansen, G.; Billeter, M. A., Rescue of 518
measles viruses from cloned DNA. *Embo J* **1995**, *14*, (23), 5773–84. 519

16. Farnes, R.; Deval, J., New antiviral approaches for respiratory syncytial virus and other mononegaviruses: Inhibiting the 520
RNA polymerase. *Antiviral Res* **2016**, *134*, 63–76. 521

17. Xie, S. Z.; Yao, K.; Li, B.; Peng, C.; Yang, X. L.; Shi, Z. L., Development of a Měnglā virus minigenome and comparison of its 522
polymerase complexes with those of other filoviruses. *Virol Sin* **2024**, *39*, (3), 459–468. 523

18. Teng, M. N.; Collins, P. L., Identification of the respiratory syncytial virus proteins required for formation and passage of 524
helper-dependent infectious particles. *J Virol* **1998**, *72*, (7), 5707–16. 525

19. Luthra, P.; Jordan, D. S.; Leung, D. W.; Amarasinghe, G. K.; Basler, C. F., Ebola virus VP35 interaction with dynein LC8 526
regulates viral RNA synthesis. *J Virol* **2015**, *89*, (9), 5148–53. 527

20. Leung, Daisy W.; Borek, D.; Luthra, P.; Binning, Jennifer M.; Anantpadma, M.; Liu, G.; Harvey, Ian B.; Su, Z.; Endlich-Frazier, 528
A.; Pan, J.; Shabman, Reed S.; Chiu, W.; Davey, Robert A.; Otwinowski, Z.; Basler, Christopher F.; Amarasinghe, Gaya K., 529
An Intrinsically Disordered Peptide from Ebola Virus VP35 Controls Viral RNA Synthesis by Modulating Nucleoprotein- 530
RNA Interactions. *Cell Reports* **2015**, *11*, (3), 376–389. 531

21. Hoenen, T., Minigenome Systems for Filoviruses. *Methods Mol Biol* **2018**, *1604*, 237–245. 532

22. Xu, W.; Luthra, P.; Wu, C.; Batra, J.; Leung, D. W.; Basler, C. F.; Amarasinghe, G. K., Ebola virus VP30 and nucleoprotein 533
interactions modulate viral RNA synthesis. *Nature Communications* **2017**, *8*, (1), 15576. 534

23. Su, Z.; Wu, C.; Shi, L.; Luthra, P.; Pintilie, G. D.; Johnson, B.; Porter, J. R.; Ge, P.; Chen, M.; Liu, G.; Frederick, T. E.; Binning, 535
J. M.; Bowman, G. R.; Zhou, Z. H.; Basler, C. F.; Gross, M. L.; Leung, D. W.; Chiu, W.; Amarasinghe, G. K., Electron Cryo- 536

microscopy Structure of Ebola Virus Nucleoprotein Reveals a Mechanism for Nucleocapsid-like Assembly. *Cell* **2018**, *172*, (5), 966–978.e12. 537

538

24. Teng, M. N.; Tran, K. C., Minigenome System to Study Respiratory Syncytial Virus Gene Expression. *Methods Mol Biol* **2025**, 2948, 97–107. 539

540

25. Yu, Q.; Hardy, R. W.; Wertz, G. W., Functional cDNA clones of the human respiratory syncytial (RS) virus N, P, and L 541

proteins support replication of RS virus genomic RNA analogs and define minimal trans-acting requirements for RNA 542

replication. *J Virol* **1995**, *69*, (4), 2412–9. 543

26. Hotard, A. L.; Shaikh, F. Y.; Lee, S.; Yan, D.; Teng, M. N.; Plemper, R. K.; Crowe, J. E., Jr.; Moore, M. L., A stabilized 544

respiratory syncytial virus reverse genetics system amenable to recombination-mediated mutagenesis. *Virology* **2012**, *434*, 545

(1), 129–36. 546

27. Schmidt, M. L.; Tews, B. A.; Groseth, A.; Hoenen, T., Generation and Optimization of a Green Fluorescent Protein- 547

Expressing Transcription and Replication-Competent Virus-Like Particle System for Ebola Virus. *The Journal of Infectious 548*

Diseases **2018**, *218*, (suppl_5), S360–S364. 549

28. Ramanathan, P.; Tigabu, B.; Santos, R. I.; Ilinskykh, P. A.; Kuzmina, N.; Vogel, O. A.; Thakur, N.; Ahmed, H.; Wu, C.; 550

Amarasinghe, G. K.; Basler, C. F.; Bukreyev, A., Ebolavirus Species-Specific Interferon Antagonism Mediated by VP24. 551

Viruses **2023**, *15*, (5), 1075. 552

29. Sutto-Ortiz, P.; Tcherniuk, S.; Ysebaert, N.; Abeywickrema, P.; Noël, M.; Decombe, A.; Debart, F.; Vasseur, J. J.; Canard, B.; 553

Roymans, D.; Rigaux, P.; Eléouët, J. F.; Decroly, E., The methyltransferase domain of the Respiratory Syncytial Virus L 554

protein catalyzes cap N7 and 2'-O-methylation. *PLoS Pathog* **2021**, *17*, (5), e1009562. 555

30. Schmidt, M. L.; Hoenen, T., Characterization of the catalytic center of the Ebola virus L polymerase. *PLoS Negl Trop Dis* **2017**, 556

11, (10), e0005996. 557

31. Tran, K. C.; Collins, P. L.; Teng, M. N., Effects of altering the transcription termination signals of respiratory syncytial virus 558

on viral gene expression and growth in vitro and in vivo. *J Virol* **2004**, *78*, (2), 692–9. 559

32. Farns, R.; Collins, P. L., Model for polymerase access to the overlapped L gene of respiratory syncytial virus. *J Virol* **1999**, 560

73, (1), 388–97. 561

33. Watt, A.; Moukambi, F.; Banadyga, L.; Groseth, A.; Callison, J.; Herwig, A.; Ebihara, H.; Feldmann, H.; Hoenen, T., A novel 562

life cycle modeling system for Ebola virus shows a genome length-dependent role of VP24 in virus infectivity. *J Virol* **2014**, 563

88, (18), 10511–24. 564

34. Hume, A. J.; Mühlberger, E., Distinct Genome Replication and Transcription Strategies within the Growing Filovirus Family. 565

J Mol Biol **2019**, *431*, (21), 4290–4320. 566

35. Bodmer, B. S.; Gressler, J.; Schmidt, M. L.; Holzerland, J.; Brandt, J.; Braun, S.; Groseth, A.; Hoenen, T., Differences in Viral 567

RNA Synthesis but Not Budding or Entry Contribute to the In Vitro Attenuation of Reston Virus Compared to Ebola Virus. 568

Microorganisms **2020**, *8*, (8). 569

36. Li, Y.; Wang, X.; Blau, D. M.; Caballero, M. T.; Feikin, D. R.; Gill, C. J.; Madhi, S. A.; Omer, S. B.; Simões, E. A. F.; Campbell, 570

H.; Pariente, A. B.; Bardach, D.; Bassat, Q.; Casalegno, J. S.; Chakhunashvili, G.; Crawford, N.; Danilenko, D.; Do, L. A. H.; 571

Echavarria, M.; Gentile, A.; Gordon, A.; Heikkinen, T.; Huang, Q. S.; Jullien, S.; Krishnan, A.; Lopez, E. L.; Markić, J.; Mira- 572

Iglesias, A.; Moore, H. C.; Moyes, J.; Mwananyanda, L.; Nokes, D. J.; Noordeen, F.; Obodai, E.; Palani, N.; Romero, C.; Salimi, 573

V.; Satav, A.; Seo, E.; Shchomak, Z.; Singleton, R.; Stolyarov, K.; Stoszek, S. K.; von Gottberg, A.; Wurzel, D.; Yoshida, L. M.; 574

Yung, C. F.; Zar, H. J.; Nair, H., Global, regional, and national disease burden estimates of acute lower respiratory infections 575

due to respiratory syncytial virus in children younger than 5 years in 2019: a systematic analysis. *Lancet* **2022**, *399*, (10340), 576

2047–2064. 577

37. Mazur, N. I.; Caballero, M. T.; Nunes, M. C., Severe respiratory syncytial virus infection in children: burden, management, 578

and emerging therapies. *The Lancet* **2024**, *404*, (10458), 1143–1156. 579

38. Jeong, Y. D.; Park, S.; Lee, S.; Jang, W.; Park, J.; Lee, K.; Lee, J.; Kang, J.; Udeh, R.; Rahmati, M.; Yeo, S. G.; Smith, L.; Lee, H.; Yon, D. K., Global burden of vaccine-associated Guillain-Barré syndrome over 170 countries from 1967 to 2023. *Sci Rep* **2024**, 14, (1), 24561. 580
581
582

39. Anderer, S., FDA Issues Warning of Guillain-Barré Syndrome Risk for 2 RSV Vaccines. *Jama* **2025**. 583

40. Du Toit, A., Evaluating an RSV inhibitor. *Nat Rev Microbiol* **2022**, 20, (5), 254. 584

41. Plackett, B., RSV treatments are here: now the work begins. *Nature* **2023**, 621, (7980), S51. 585

42. Wei, X.; Wang, L.; Li, M.; Qi, J.; Kang, L.; Hu, G.; Gong, C.; Wang, C.; Wang, Y.; Huang, F.; Gao, G. F., Novel imported clades accelerated the RSV surge in Beijing, China, 2023–2024. *J Infect* **2024**, 89, (6), 106321. 586
587

43. Fu, Y.-H.; Liu, Y.-R.; Zheng, Y.-P.; Jiang, N.; Yue Ying, J.; Li, W.; Peng, X.-L.; He, J.-S., An RNA polymerase I-driven human respiratory syncytial virus minigenome as a tool for quantifying virus titers and screening antiviral drug. *Chinese Chemical Letters* **2017**, 28, (1), 131–135. 588
589
590

44. Teng, M. N.; Tran, K. C., Use of Minigenome Systems to Study RSV Transcription. *Methods Mol Biol* **2016**, 1442, 155–64. 591

45. Stepanenko, O. V.; Sulatsky, M. I.; Mikhailova, E. V.; Kuznetsova, I. M.; Turoverov, K. K.; Stepanenko, O. V.; Sulatskaya, A. I., New findings on GFP-like protein application as fluorescent tags: Fibrillogenesis, oligomerization, and amorphous aggregation. *Int J Biol Macromol* **2021**, 192, 1304–1310. 592
593
594

46. Kang, Y. S.; Kirby, J. E., A Versatile Nanoluciferase Reporter Reveals Structural Properties Associated with a Highly Efficient, N-Terminal *Legionella pneumophila* Type IV Secretion Translocation Signal. *Microbiol Spectr* **2023**, 11, (2), e0233822. 595
596

47. Pandya, M. C.; Callahan, S. M.; Savchenko, K. G.; Stobart, C. C., A Contemporary View of Respiratory Syncytial Virus (RSV) Biology and Strain-Specific Differences. *Pathogens* **2019**, 8, (2). 597
598

48. Gilman, M. S. A.; Liu, C.; Fung, A.; Behera, I.; Jordan, P.; Rigaux, P.; Ysebaert, N.; Tcherniuk, S.; Sourimant, J.; Eléouët, J. F.; Sutto-Ortiz, P.; Decroly, E.; Roymans, D.; Jin, Z.; McLellan, J. S., Structure of the Respiratory Syncytial Virus Polymerase Complex. *Cell* **2019**, 179, (1), 193–204.e14. 599
600
601

49. Cao, D.; Gao, Y.; Roesler, C.; Rice, S.; D'Cunha, P.; Zhuang, L.; Slack, J.; Domke, M.; Antonova, A.; Romanelli, S.; Keating, S.; Forero, G.; Juneja, P.; Liang, B., Cryo-EM structure of the respiratory syncytial virus RNA polymerase. *Nat Commun* **2020**, 11, (1), 368. 602
603
604

50. Noton, S. L.; Tremaglio, C. Z.; Fearn, R., Killing two birds with one stone: How the respiratory syncytial virus polymerase initiates transcription and replication. *PLoS Pathog* **2019**, 15, (2), e1007548. 605
606

51. Sourimant, J.; Lieber, C. M.; Yoon, J. J.; Toots, M.; Govindarajan, M.; Uduumula, V.; Sakamoto, K.; Natchus, M. G.; Patti, J.; Vernachio, J.; Plemper, R. K., Orally efficacious lead of the AVG inhibitor series targeting a dynamic interface in the respiratory syncytial virus polymerase. *Sci Adv* **2022**, 8, (25), eab02236. 607
608
609

52. Liuzzi, M.; Mason, S. W.; Cartier, M.; Lawetz, C.; McCollum, R. S.; Dansereau, N.; Bolger, G.; Lapeyre, N.; Gaudette, Y.; Lagacé, L.; Massariol, M. J.; Dô, F.; Whitehead, P.; Lamarre, L.; Scouten, E.; Bordeleau, J.; Landry, S.; Rancourt, J.; Fazal, G.; Simoneau, B., Inhibitors of respiratory syncytial virus replication target cotranscriptional mRNA guanylylation by viral RNA-dependent RNA polymerase. *J Virol* **2005**, 79, (20), 13105–15. 610
611
612
613

53. Fearn, R.; Peebles, M. E.; Collins, P. L., Increased expression of the N protein of respiratory syncytial virus stimulates minigenome replication but does not alter the balance between the synthesis of mRNA and antigenome. *Virology* **1997**, 236, (1), 188–201. 614
615
616

54. Mehedi, M.; Hoenen, T.; Robertson, S.; Ricklefs, S.; Dolan, M. A.; Taylor, T.; Falzarano, D.; Ebihara, H.; Porcella, S. F.; Feldmann, H., Ebola virus RNA editing depends on the primary editing site sequence and an upstream secondary structure. *PLoS Pathog* **2013**, 9, (10), e1003677. 617
618
619

55. Prins, K. C.; Binning, J. M.; Shabman, R. S.; Leung, D. W.; Amarasinghe, G. K.; Basler, C. F., Basic residues within the ebolavirus VP35 protein are required for its viral polymerase cofactor function. *J Virol* **2010**, 84, (20), 10581–91. 620
621
622